Materials Research Proceedings 31 (2023) 99-108 https://doi.org/10.21741/9781644902592-11

The flexoelectric effect for interface cracks between two dissimilar materials

Tomas Profant[1,2,a] , Jan Sladek[1,b] , and Vladimir Sladek[1,c*]

[1]Institute of Construction and Architecture, Slovak Academy of Sciences, 84503 Bratislava, Slovakia

[2]Institute of Solid Mechanics, Brno University of Technology, Technicka 2, 61669 Brno, Czech Republic

[a]profant@fme.vutbr.cz, [b]jan.sladek@savba.sk, [c]vladimir.sladek@savba.sk

Keywords: Dielectric Material, Gradient Theory, Flexoelectricity, Asymptotic Solution, Mixed FEM

Abstract. It is developed the procedure of the assessment of the amplitude factors in the asymptotic solution for the interface crack between two flexoelectric materials. The stress exponents with the appropriate eigenvectors of the regular and auxiliary solutions are evaluated from the eigenvalue problem assembled from the boundary conditions prevailing at the tip of the crack. The amplitude factors of the asymptotic solution are computed from the two-state integrals in which the regular, auxiliary, and finite element solution represent the independent equilibrium states. The obtained results show the capability of the two-state integrals to extract the dominant terms of the asymptotic solution from the weak solution of the fracture problem represented by the finite element method. The amplitude factors representing the most singular terms of the asymptotic solution at the crack tip are quantities playing an important role in the problems of crack stability criterions.

Introduction

The influence of the flexoelectricity on behaviour of the interface crack between two dissimilar dielectric materials under a mechanical load is investigated in the present paper. The direct flexoelectricity is an electro-mechanical coupling phenomenon, where the electric polarization is induced by a strain gradient in dielectrics [1-3]. For a long time, the polarization has been observed in nature only in non-centrosymmetric arrangement of atoms in crystals and this effect is called as piezoelectricity. After experimental discovery of flexoelectricity, we can see that strain gradients may break the inversion symmetry in centrosymmetric crystals and electric polarization might be observed in all dielectric materials. A significant flexoelectricity is expected at the crack tip vicinity, where the strain gradients are large [2,3]. Earlier research results showed a strong influence of the strain gradients on fields at the crack tip vicinity and the finite value of the Cauchy stresses at the crack tip contrary to the classical elasticity [4], if strain gradients are considered in constitutive equations. Gourgiotis and Georgiadis [4] derived asymptotic expressions for stress and displacement fields around the crack tip within a strain gradient continuum model. Recently, authors [5] have derived asymptotic fields at the crack tip vicinity in a homogeneous material with a direct flexoelectric effect.

Layered composite structures are frequently employed in engineering to utilize excellent properties of individual constituents. Due to a poor adhesion of layers, the interface crack can often be observed there. Therefore, behaviour of interface cracks should be studied to increase the safety of layered structures. Gradient theories better describe fields at the crack tip vicinity since they consider large strain gradients counterpart to conventional continuum models. The flexoelectric phenomenon affects the mechanical fields and appeared also to be helpful in the self-repairing of

the human bones [5]. In the present paper, asymptotic expressions for displacements, electric potentials, stresses at the crack tip vicinity are derived for an interface crack between two dissimilar dielectric materials under the crack mode I. The asymptotic expansion method is applied to get these expressions. The results for asymptotic field distributions are compared with numerical results obtained by the mixed finite element method (FEM) [6].

Governing equations

It is considered an isotropic dielectric solid with direct flexoelectricity effect. Because of the size dependency and electro-mechanical coupling [7], the constitutive equations must combine the infinitesimal strain tensor ε_{ij}, its gradient η_{ijk} and the electric field E_i. These are defined as $\varepsilon_{ij} = (u_{i,j} + u_{j,i})/2$, $\eta_{ijk} = \varepsilon_{ij,k}$ and $E_i = -\varphi_{,i}$, where u_i is the displacement vector and φ is the electric potential. The isotropic flexoelectric solid is characterized by the Lamé coefficients λ and μ, the length scale parameter l, two flexoelectric constants f_1 and f_2, and the dielectric permittivity κ. The following form of the constitutive equations describe all these circumstances [8],

$$\sigma_{ij} = \lambda\varepsilon_{ll}\delta_{ij} + 2\mu\varepsilon_{ij}, \tag{1}$$
$$\tau_{ijk} = l^2\left(\lambda\varepsilon_{ll,k}\delta_{ij} + 2\mu\varepsilon_{ij,k}\right) - f_1E_k\delta_{ij} - f_2E_i\delta_{jk} - f_2E_j\delta_{ik}, \tag{2}$$
$$D_i = \kappa E_i + f_1\varepsilon_{ll,i} + 2f_2\varepsilon_{li,l}, \tag{3}$$

where the Einstein notation is used, σ_{ij} is the Cauchy stress tensor, τ_{ijk} is the higher order stress tensor, D_i is the electric displacement vector and δ_{ij} is the Kronecker delta. The governing equations inside a domain Ω are [7-9]

$$\sigma_{il,l} - \tau_{ilm,lm} = 0, \tag{4}$$
$$D_{l,l} = 0 \tag{5}$$

with the associated essential boundary conditions

$$u_i = \overline{u}_i \text{ on } \partial\Omega_u, \tag{6}$$
$$\varphi = \overline{\varphi} \text{ on } \partial\Omega_\varphi \tag{7}$$
$$v_i = u_{i,l}n_l = \overline{v}_i \text{ on } \partial\Omega_v, \tag{8}$$

or the natural boundary equations

$$t_i = n_l\left(\sigma_{il} - \tau_{ilm,m}\right) - \pi_l\rho_{i,l} + \sum_c|\rho_i(\boldsymbol{x}^c)|\delta(\boldsymbol{x} - \boldsymbol{x}^c) = \overline{t}_i \text{ on } \partial\Omega_t, \tag{9}$$
$$R_i = n_ln_m\tau_{ilm} = \overline{R}_i \text{ on } \partial\Omega_R, \tag{10}$$
$$Q = n_lD_l = \overline{Q} \text{ on } \partial\Omega_Q. \tag{11}$$

Besides modification of the classical elasticity expression for traction vector $\boldsymbol{t_i}$ in considered model used in classical elasticity, there are also additional boundary densities in our mathematical model, such as the normal derivative of displacements $\boldsymbol{v_i}$, traction vector of the higher order of stresses $\boldsymbol{R_i}$ and electric charge $\boldsymbol{Q}$. The vectors $\boldsymbol{n_i}$ and $\boldsymbol{\pi_i}$ are the unit normal and tangent, respectively, on the boundary $\boldsymbol{\partial\Omega}$. The sum in Eq. 9 means the jumps at possible corners $\boldsymbol{c}$ on the boundary $\boldsymbol{\partial\Omega}$ with magnitude

$$|\rho_i(\boldsymbol{x}^c)| = \rho_i(\boldsymbol{x}^c - 0) - \rho_i(\boldsymbol{x}^c + 0), \tag{12}$$

where $\boldsymbol{\rho_i} = \boldsymbol{n_l\pi_m\tau_{ilm}}$. It is worth to note that $\boldsymbol{\partial\Omega_u \cup \partial\Omega_t = \partial\Omega_v \cup \partial\Omega_R = \partial\Omega_\varphi \cup \partial\Omega_Q = \partial\Omega}$ and $\boldsymbol{\partial\Omega_u \cap \partial\Omega_t = \partial\Omega_v \cap \partial\Omega_R = \partial\Omega_\varphi \cap \partial\Omega_Q = \emptyset}$ must be satisfied. The substituting of the

constitutive equations Eq. 1-Eq. 3 to the governing equations Eq. 4 and Eq. 5 allows one to derive the following Navier-type equations, written in the vector form [8]

$$\Delta[\kappa\varphi + f\mathrm{div}(\boldsymbol{u})] = 0, \tag{13}$$
$$(\lambda+\mu)(1-l_1^2\Delta)\mathrm{grad}\big(\mathrm{div}(\boldsymbol{u})\big) + \mu(1-l^2\Delta)\Delta\boldsymbol{u} = 0, \tag{14}$$

where Δ is the Laplacian operator, $f = f_1 + 2f_2$ and

$$l_1^2 = l^2 + f^2\kappa^{-1}(\lambda+\mu)^{-1}. \tag{15}$$

Recall that f and l_1 are used just for abbreviation and they are not extra material coefficients.

General asymptotic solution

A standard Knein-Williams asymptotic technique [4,10,11] is employed to establish the general solution of the stress, displacement and electric field at the crack tip vicinity with consideration of large strain gradients. It is necessary to implement the polar coordinate system (r,θ) at the crack tip and consider the distance from it so small $(r \to 0)$ that only the dominant part of Eq. 14 can be retained

$$(\lambda+\mu)l_1^2\Delta\big[\mathrm{grad}\big(\mathrm{div}(\boldsymbol{u})\big)\big] + \mu l^2\Delta(\Delta\boldsymbol{u}) = 0. \tag{16}$$

The solution of Eq. 13 and Eq. 16 for displacement components and electric potential, u_r, u_θ and φ, respectively, are found as an asymptotic series of separated variable terms

$$u_r = r^p\{A_1\cos(p-1)\theta + B_1\sin(p-1)\theta + A_2\cos(p+1)\theta + B_2\sin(p+1)\theta + A_3\cos(p-3)\theta + B_3\sin(p-3)\theta\}, \tag{17}$$
$$u_\theta = r^p\{B_4\cos(p-1)\theta + A_4\sin(p-1)\theta + B_2\cos(p+1)\theta - A_2\sin(p+1)\theta + \gamma[B_3\cos(p-3)\theta - A_3\sin(p-3)\theta]\}, \tag{18}$$
$$\varphi = r^{p-1}\kappa^{-1}\{E_1\cos(p-1)\theta + F_1\sin(p-1)\theta\} + \kappa^{-1}f\mathrm{div}(\boldsymbol{u}), \tag{19}$$

where

$$\gamma = \frac{l_1^2(p+1)(\lambda+\mu)+4l^2\mu}{l_1^2(p-3)(\lambda+\mu)-4l^2\mu}. \tag{20}$$

The exponent p and the coefficients A_i and B_i are generally complex. Consequently, the solution with their complex conjugate values also satisfies Eq. 13 and Eq. 16 and the real valued solution is the superposition of both ones. It can be simply verified that the solution with exponent $p^* = 2 - p$ and corresponding coefficients A_i^* and B_i^* also satisfies Eq. 13 and Eq. 16. This solution is so-called auxiliary solution and it plays an important role in the evaluation procedure of the regular coefficients A_i and B_i.

Asymptotic solution for an interface crack

Let the interface semi-infinite crack lies along the negative x axis and the polar coordinate system (r,θ) is introduced to its tip. The material in the upper half plane $y > 0$ is denoted by the superscript I and the material in the lower half plane $y < 0$ is denoted by the superscript II. The asymptotic solutions Eq. 17 and Eq. 18 for both materials can be rewritten to the matrix form

$$\boldsymbol{u}^{I,II} = r^p\big\{\boldsymbol{U}_a^{I,II}(\theta;p)\boldsymbol{a}^{I,II} + \boldsymbol{U}_b^{I,II}(\theta;p)\boldsymbol{b}^{I,II}\big\}, \tag{21}$$

where

$$\boldsymbol{a}^{I,II} = \left[A_1^{I,II}, A_2^{I,II}, A_3^{I,II}, A_4^{I,II}, E_1^{I,II}\right]^T, \boldsymbol{b}^{I,II} = \left[B_1^{I,II}, B_2^{I,II}, B_3^{I,II}, B_4^{I,II}, F_1^{I,II}\right]^T \tag{22}$$

and

$$\boldsymbol{U}_a^{I,II}(\theta;p) = \begin{bmatrix} \cos(p-1)\theta & \cos(p+1)\theta & \cos(p-3)\theta & 0 & 0 \\ 0 & -\sin(p+1)\theta & -\gamma^{I,II}\sin(p-3)\theta & \sin(p-1)\theta & 0 \end{bmatrix}, \tag{23}$$

$$\boldsymbol{U}_b^{I,II}(\theta;p) = \begin{bmatrix} \sin(p-1)\theta & \sin(p+1)\theta & \sin(p-3)\theta & 0 & 0 \\ 0 & \cos(p+1)\theta & \gamma^{I,II}\cos(p-3)\theta & \cos(p-1)\theta & 0 \end{bmatrix}. \tag{24}$$

Similarly the electric potential φ^J from Eq. 19 and remaining densities $\boldsymbol{v}^J$, $\boldsymbol{t}^J$, $\boldsymbol{R}^J$ and Q^J in Eq. 8-Eq. 11 can be written as

$$\varphi^{I,II} = r^{p-1}\left\{\boldsymbol{\phi}_a^{I,II}(\theta;p)\boldsymbol{a}^{I,II} + \boldsymbol{\phi}_b^{I,II}(\theta;p)\boldsymbol{b}^{I,II}\right\}, \tag{25}$$

$$\boldsymbol{v}^{I,II} = r^{p-1}\left\{\boldsymbol{V}_a^{I,II}(\theta;p)\boldsymbol{a}^{I,II} + \boldsymbol{V}_b^{I,II}(\theta;p)\boldsymbol{b}^{I,II}\right\}, \tag{26}$$

$$\boldsymbol{t}^{I,II} = r^{p-3}\left\{\boldsymbol{T}_a^{I,II}(\theta;p)\boldsymbol{a}^{I,II} + \boldsymbol{T}_b^{I,II}(\theta;p)\boldsymbol{b}^{I,II}\right\}, \tag{27}$$

$$\boldsymbol{R}^{I,II} = r^{p-2}\left\{\boldsymbol{R}_a^{I,II}(\theta;p)\boldsymbol{a}^{I,II} + \boldsymbol{R}_b^{I,II}(\theta;p)\boldsymbol{b}^{I,II}\right\}, \tag{28}$$

$$Q^{I,II} = r^{p-2}\left\{\boldsymbol{q}_a^{I,II}(\theta;p)\boldsymbol{a}^{I,II} + \boldsymbol{q}_b^{I,II}(\theta;p)\boldsymbol{b}^{I,II}\right\}. \tag{29}$$

The vectors $\boldsymbol{\phi}_{a,b}^{I,II}(\theta;p)$, $\boldsymbol{q}_{a,b}^{I,II}(\theta;r)$ and matrices $\boldsymbol{V}_{a,b}^{I,II}(\theta;p)$, $\boldsymbol{T}_{a,b}^{I,II}(\theta;p)$, $\boldsymbol{R}_{a,b}^{I,II}(\theta;p)$ are not shown here due to their complexity. The boundary conditions for the traction-free and isolated crack faces at $\theta = \pm\pi$ of material I and II are

$$\boldsymbol{t}^I(r,\pi) = \boldsymbol{R}^I(r,\pi) = 0 \text{ and } Q^I(r,\pi) = 0, \tag{30}$$

$$\boldsymbol{t}^{II}(r,-\pi) = \boldsymbol{R}^{II}(r,-\pi) = 0 \text{ and } Q^{II}(r,-\pi) = 0 \tag{31}$$

with compatibility conditions along the interface for $\theta = 0$

$$\boldsymbol{u}^I(r,0) = \boldsymbol{u}^{II}(0;p),\ \varphi^I(r,0) = \varphi^{II}(r,0),\ \boldsymbol{v}^I(r,0) = -\boldsymbol{v}^{II}(r,0), \tag{32}$$

$$\boldsymbol{t}^I(r,0) = -\boldsymbol{t}^{II}(r,0),\ \boldsymbol{R}^I(r,0) = \boldsymbol{R}^{II}(r,0),\ Q^I(r,0) = -Q^{II}(r,0). \tag{33}$$

The substitution of Eq. 21 and Eq. 25-Eq. 29 into Eq. 30-Eq. 33 can be written formally as follows

$$\boldsymbol{B}^{I,II}(p)\boldsymbol{g}^{I,II} = 0, \tag{34}$$

$$\boldsymbol{C}^I(p)\boldsymbol{g}^I = \boldsymbol{C}^{II}(p)\boldsymbol{g}^{II}, \tag{35}$$

where $\boldsymbol{g}^{I,II} = [\boldsymbol{a}^{I,II}, \boldsymbol{b}^{I,II}]^T$ and

$$\boldsymbol{B}^{I,II}(p) = \begin{bmatrix} \boldsymbol{T}_a^{I,II}(\pm\pi;p) & \boldsymbol{T}_b^{I,II}(\pm\pi;p) \\ \boldsymbol{R}_a^{I,II}(\pm\pi;p) & \boldsymbol{R}_b^{I,II}(\pm\pi;p) \\ q_a^{I,II}(\pm\pi;p) & q_b^{I,II}(\pm\pi;p) \end{bmatrix}, \boldsymbol{C}^{I,II}(p) = \begin{bmatrix} \boldsymbol{U}_a^{I,II}(0;p) & \boldsymbol{U}_b^{I,II}(0;p) \\ \boldsymbol{\phi}_b^{I,II}(0;p) & \boldsymbol{\phi}_b^{I,II}(0;p) \\ \boldsymbol{V}_b^{I,II}(0;p) & \boldsymbol{V}_b^{I,II}(0;p) \\ \boldsymbol{T}_a^{I,II}(0;p) & \boldsymbol{T}_b^{I,II}(0;p) \\ \boldsymbol{R}_a^{I,II}(0;p) & \boldsymbol{R}_b^{I,II}(0;p) \\ q_a^{I,II}(0;p) & q_b^{I,II}(0;p) \end{bmatrix}. \tag{36}$$

The relations Eq. 35 allow one to establish the following eigenvalue problem

$$\boldsymbol{A}(p)\boldsymbol{g}^{I} = 0, \tag{37}$$

in which

$$\boldsymbol{A}(p) = \begin{bmatrix} \boldsymbol{B}^{I}(p) \\ \boldsymbol{B}^{II}(p)[\boldsymbol{C}^{II}(p)]^{-1}\boldsymbol{C}^{I}(p) \end{bmatrix}. \tag{38}$$

The condition for the existence of the nontrivial solution of Eq. 37 is

$$\det[A(p)] = 0, \tag{39}$$

which is the characteristic equation for the complex exponent p. It is worth to note that the most singular admissible real value of the exponent p is $\Re\{p\} = 3/2$ or $1 < p < 2$ in the case of real p. This is due to the requirement of the finite value of the potential energy of the cracked bimaterial. The eigenvalue $p = 1$ also satisfies Eq. 39, but the corresponding lower-order terms Eq. 17-Eq. 18 and their counterparts Eq. 1-Eq. 3 do not contribute to the J-integral and to the crack opening displacement [4]. Taking into account the lower-order and the most singular terms, the regular solution for displacement and electric field for material I and II and for $r \to 0$ can be written as

$$\begin{aligned} &\boldsymbol{u}^{I,II} = r\{\Gamma_1^{I,II} + \Gamma_2^{I,II}\cos 2\theta + \Gamma_3^{I,II}\sin 2\theta\} + H_0 r^{p_0}\{\boldsymbol{U}_a^{I,II}(\theta;p_0)\boldsymbol{a}_0^{I,II} + \boldsymbol{U}_b^{I,II}(\theta;p_0)\boldsymbol{b}_0^{I,II}\} + \\ &\sum_{i=1}^{4} H_i r^{p_i}\{\boldsymbol{U}_a^{I,II}(\theta;p_i)\boldsymbol{a}_i^{I,II} + \boldsymbol{U}_b^{I,II}(\theta;p_i)\boldsymbol{b}_i^{I,II}\} = r\{\Gamma_1^{I,II} + \Gamma_2^{I,II}\cos 2\theta + \Gamma_3^{I,II}\sin 2\theta\} + \\ &\sum_{0}^{4} H_i \boldsymbol{G}_i^{I,II}(r,\theta;p_i), \end{aligned} \tag{40}$$

$$\begin{aligned} &\varphi^{I,II} = \kappa^{-1}\Gamma_0^{I,II} + H_0 r^{p_0-1}\{\boldsymbol{\phi}_a^{I,II}(\theta;p_0)\boldsymbol{a}_0^{I,II} + \boldsymbol{\phi}_b^{I,II}(\theta;p_0)\boldsymbol{b}_0^{I,II}\} + \\ &\sum_{i=1}^{4} H_i r^{p_i-1}\{\boldsymbol{\phi}_a^{I,II}(\theta;p_i)\boldsymbol{a}_i^{I,II} + \boldsymbol{\phi}_a^{I,II}(\theta;p_i)\boldsymbol{b}_i^{I,II}\} + (\kappa^{I,II})^{-1} f^{I,II}\mathrm{div}(\boldsymbol{u}^{I,II}) = \kappa^{-1}\Gamma_0^{I,II} + \\ &\sum_{i=0}^{4} H_i F_i^{I,II}(r,\theta;p_i), \end{aligned} \tag{41}$$

where H_0 and H_i are unknow amplitude factors. Except the exponent $p_0 = 3/2$, the remaining ones p_i can be real or complex with their conjugates. The eigenvectors $\boldsymbol{a}_i^{I,II}$ and $\boldsymbol{b}_i^{I,II}$ for $i = 0,1,\dots,4$ are obtained from the eigenvalue problem Eq. 37 and consequently from the relation Eq. 35 after the back substitution of the associated exponents p_i. The factors $\Gamma_i^{I,II}$ for $i = 0,\dots,3$ are evaluated from the finite values of the electric potential and components of the Cauchy stresses given by Eq. 1 at the tip of the crack as follows [12]

$$\Gamma_0^{I,II} = (\kappa^{I.II})^{-1}\varphi^{I,II}|_{r=0} - 2f^{I,II}\Gamma_1^{I,II}, \tag{42}$$

$$\Gamma_1^{I,II} = \frac{\left(\sigma_{xx}^{I,II}+\sigma_{yy}^{I,II}\right)\big|_{r=0}}{4(\lambda^{I,II}+\mu^{I,II})},\ \Gamma_2^{I,II} = \frac{\left(\sigma_{xx}^{I,II}-\sigma_{yy}^{I,II}\right)\big|_{r=0}}{4\mu^{I,II}},\ \Gamma_3 = \frac{\sigma_{xy}^{I,II}\big|_{r=0}}{2\mu^{I,II}}. \tag{43}$$

Although the case $p < 1$ is excluded from the regular solution, the so-called auxiliary solutions including the exponents $p_i^* = 2 - p_i$ for $i = 0,1,\dots,4$ are also taken into account in the following and can written in the form

$$\boldsymbol{u}_i^{*I,II} = r^{p_i^*}\{\boldsymbol{U}_a^{I,II}(\theta;p_i^*)\boldsymbol{a}_i^{*I,II} + \boldsymbol{U}_b^{I,II}(\theta;p_i^*)\boldsymbol{b}_i^{*I,II}\}, \tag{44}$$

$$\varphi_i^{*I,II} = r^{p_i^*-1}\{\boldsymbol{\phi}_a^{I,II}(\theta;p_i^*)\boldsymbol{a}_i^{*I,II} + \boldsymbol{\phi}_a^{I,II}(\theta;p_i^*)\boldsymbol{b}_i^{*I,II}\} + (\kappa^{I,II})^{-1} f^{I,II}\mathrm{div}(\boldsymbol{u}^{*I,II}). \tag{45}$$

The auxiliary solutions Eq. 44 and Eq. 45 are the mathematical tool that plays a key role in the evaluation of the amplitude factors H_i that appear in the asymptotic solution Eq. 40 and Eq. 41. They can extract the magnitude of the amplitude factors H_i from the exact complete solution of

the interface crack problem through the Betti contour integral. The extension of the Betti's reciprocal theorem to the direct flexoelectricity problem is derived in [13].

Two-state integrals

Assuming that the body forces are absent, the two-state integral as the consequence of the Betti reciprocal theorem [13] can be defined as

$$\mathcal{H}\left(\boldsymbol{u}^{(1)},\varphi^{(1)};\boldsymbol{u}^{(2)},\varphi^{(2)}\right)=\int_{\Gamma}[\boldsymbol{t}^{(1)}\cdot\boldsymbol{u}^{(2)}+\boldsymbol{R}^{(1)}\cdot\boldsymbol{v}^{(2)}-\varphi^{(1)}Q^{(2)}-\boldsymbol{t}^{(2)}\cdot\boldsymbol{u}^{(1)}-\boldsymbol{R}^{(2)}\cdot\boldsymbol{v}^{(1)}+\varphi^{(2)}Q^{(1)}]\mathrm{d}\Gamma, \tag{46}$$

where the dot symbol means the dot product of the vectors. Two sets of forces $\left(\boldsymbol{t}^{(1)},\boldsymbol{R}^{(1)},Q^{(1)}\right)$ and $\left(\boldsymbol{t}^{(2)},\boldsymbol{R}^{(2)},Q^{(2)}\right)$ act through kinematical fields $\left(\boldsymbol{u}^{(1)},\boldsymbol{v}^{(1)},\varphi^{(1)}\right)$ and $\left(\boldsymbol{u}^{(2)},\boldsymbol{v}^{(2)},\varphi^{(2)}\right)$, respectively, along the closed smooth contour Γ in a linear elastic planar body. The two-state integral Eq. 46 is path independent [13] in the case, when the path Γ encircles the crack tip. Consider the first state $\mathcal{H}\left(\boldsymbol{u}^{I,II},\varphi^{I,II};\boldsymbol{u}_i^{*I,II},\varphi_i^{*I,II}\right)$ of integral Eq. 46 is to be evaluated on the integration path shrunk to the tip of the crack, in which the exact solutions $\boldsymbol{u}^{(1)}$ and $\varphi^{(1)}$ are approximated by the asymptotic solutions $\boldsymbol{u}^{I,II}$ and $\varphi^{I,II}$ from Eq. 40 and Eq. 39, respectively. Next, the second state $\mathcal{H}\left(\boldsymbol{u}^{h},\varphi^{h};\boldsymbol{u}_i^{*I,II},\varphi_i^{*I,II}\right)$ of integral Eq. 46 is evaluated along the remote integration path Γ and the exact solution $\boldsymbol{u}^{(1)}$ and $\varphi^{(1)}$ is approximated by a finite element solution $\boldsymbol{u}^{h}$ and φ^{h} from [7]. The auxiliary solution $\boldsymbol{u}_i^{*I,II}$ and $\varphi_i^{*I,II}$ from Eq. 44 and Eq. 45 are substituted for $\boldsymbol{u}^{(2)}$ and $\varphi^{(2)}$ in both states, respectively. Then, due to the integral path independency, both states of integral Eq. 46 must give the same value [13], i.e.

$$\mathcal{H}\left(\boldsymbol{u}^{I,II},\varphi^{I,II};\boldsymbol{u}_i^{*I,II},\varphi_i^{*I,II}\right)=\mathcal{H}\left(\boldsymbol{u}^{h},\varphi^{h};\boldsymbol{u}_i^{*I,II},\varphi_i^{*I,II}\right)\text{ for }i=0,1,\ldots,4. \tag{47}$$

The auxiliary solution Eq. 44 and Eq.45 appropriate to the exponent $p_i^*=2-p_i$ in the integral on the left-hand side of Eq. 47 causes that all terms of the asymptotic solutions Eq. 40 and Eq. 41 vanish except those with argument p_i. Consequently, the amplitude factor H_i can be extracted from the integral on the left-hand side of Eq. 47 and evaluated as

$$H_i=\frac{\mathcal{H}\left(\boldsymbol{u}^{h},\varphi^{h};\boldsymbol{u}_i^{*I,II},\varphi_i^{*I,II}\right)}{\mathcal{H}\left(\boldsymbol{G}_i^{I,II}(r,\theta;p_i),F_i^{I,II}(r,\theta;p_i);\boldsymbol{u}_i^{*I,II},\varphi_i^{*I,II}\right)}. \tag{48}$$

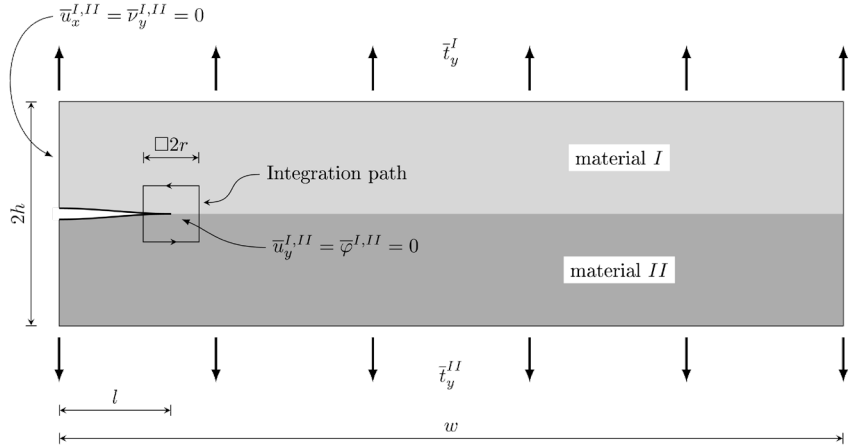

Figure 1: A symmetric part of the cracked strip under a uniform axial tension.

Materials Research Proceedings 31 (2023) 99-108 https://doi.org/10.21741/9781644902592-11

Table 1: The characteristics of the bimaterial

	material *I*	**material *II***
λ [Pa]	7.40×10^{10}	8.88×10^{10}
μ [Pa]	2.56×10^{10}	3.07×10^{10}
l [m]	1.00×10^{-8}	0.80×10^{-8}
κ [$C^2N^{-1}m^{-2}$]	1.50×10^{-8}	1.80×10^{-8}
f_1 [Cm^{-1}]	1.00×10^{-9}	0.80×10^{-9}
f_2 [Cm^{-1}]	0	0

Numerical results

It is considered a plane fracture problem of the of the bimaterial strip $2h \times 2w$ under the $\overline{t}_y^{I,II}$ external loadings with the interfacial crack whose length is $2l$. Due to the symmetry, the right half of the strip is taken into account only, as it is shown in Fig. 1. The dimensions of the crack and the strip are $l = h = 1 \times 10^{-7}$ m and $w = 1.25 \times 10^{-6}$ m. The material properties of the bimaterial are given in Tab. 1 and the external loading is $\overline{t}_y^I = \overline{t}_y^{II} = 1 \times 10^7$ Pa. The shape of the integration path in the amplitude factor evaluation procedure influences the quality of the final numerical results due to the higher-order derivatives with respect to normal $\boldsymbol{n}$ appearing in the expressions of Eq. 9. Hence, the FEM approximations of modified traction vector $\boldsymbol{t}^{I,II}$ and traction vector of the higher order of stresses $\boldsymbol{R}^{I,II}$ along the rectangular integration path, as it is shown in Fig. 1, significantly increase the accuracy of further numerical calculations.

The real and imaginary part of the characteristic function $f(p) \equiv \det[A(p)]$ for $\Re\{p\} = 3/2$ is depicted in Fig. 2, where the condition Eq. 39 is fulfilled at the intersections of both curves on the axis representing $\Im\{p\}$. These intersections give one real and two pairs of complex conjugate exponents p_i for $i = 0,1, \dots ,4$, which are given in Tab. 2. The insertion of p_i into Eq. 35 and Eq. 37 leads to the evaluation of the associated eigenvectors $\boldsymbol{g}_i^I$ and $\boldsymbol{g}_i^{II}$ for $i = 0,1, \dots ,4$ for both materials of the strip. It is worth noting that the auxiliary eigenvectors $\boldsymbol{g}_i^{*I}$ and $\boldsymbol{g}_i^{*II}$ are established in the same way as the regular ones.

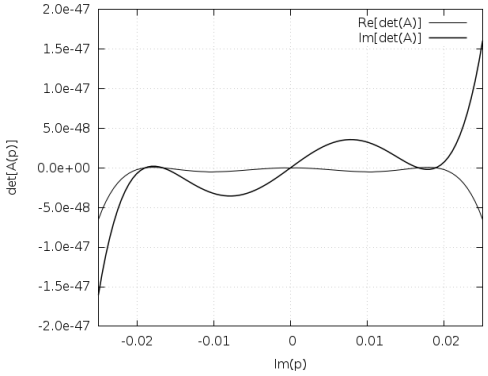

Figure 2: The real and imaginary part of the characteristic function $f(p) \equiv det[A(p)]$ for $\Re\{p\} = 3/2$.

The knowledge of exponents p_i and regular eigenvectors $\boldsymbol{g}_i^I$, $\boldsymbol{g}_i^{II}$ as well as the auxiliary eigenvectors $\boldsymbol{g}_i^{*I}$ and $\boldsymbol{g}_i^{*II}$ for $i = 0,1, \dots ,4$ and the FEM approximations of $\boldsymbol{u}^h$ and φ^h, allows one to evaluate the amplitude factors H_i applying the formulae Eq. 48. For the chosen external loading $\overline{t}_y^I = \overline{t}_y^{II} = 1 \times 10^7$ Pa the appropriate values of H_i for $i = 0,1, \dots ,4$ are calculated on the

rectangular path Γ enclosing the crack in the distance $r = 4 \times 10^{-9}$ m from its tip, as it shows Fig. 1.

Table 2: Exponents of the regular asymptotic solution.

p_0	1.500
p_1, p_2	$1.500 \pm i1.891 \times 10^{-2}$
p_3, p_4	$1.500 \pm i1.663 \times 10^{-2}$

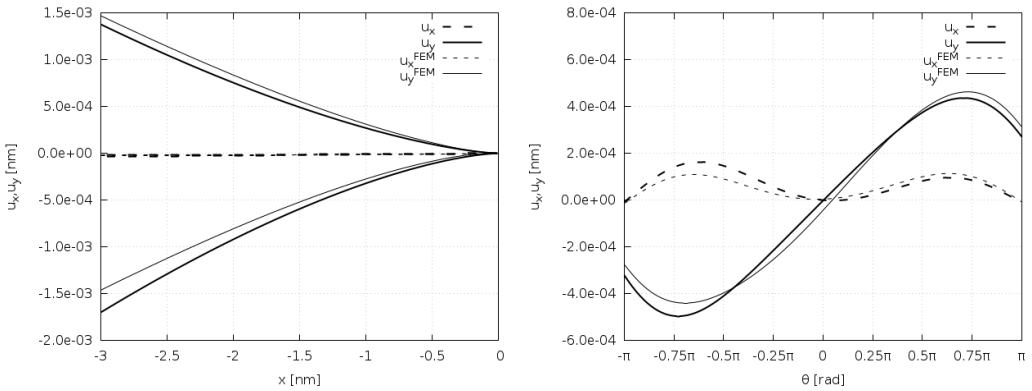

Figure 3: The crack opening displacements of the asymptotic solution and FEM solution at the right crack tip.

The comparison of the asymptotic and FEM solution of the components of the displacement vector u_x and u_y, components of Cauchy stress tensor σ_{xx}, σ_{xy} and σ_{yy} and electric potential φ in front of the crack and in the distance $r = 1 \times 10^{-9}$ m from its tip is shown in Fig. 3-Fig. 5. There is very good agreement between the asymptotic and FEM solution. On the other hand, the mismatch appears between the asymptotic and the FEM solution for increasing distance $r = x$ from the crack tip, especially for electric potential φ. This is because of the construction of the asymptotic solution Eq. 40 and Eq. 41. They are derived from the Eq. 13 and Eq. 16 at the point in whose enclosing domain the strain gradients prevail. Moreover, only the most singular terms of the asymptotic solution are taken into account. In points far from the crack tip vicinity there are significant also non-singular terms which are not considered in the asymptotic solution. The graphs in Fig. 3-Fig. 5. show that this assumption is fulfilled very close to the crack tip. The higher order terms should be added to the asymptotic solution Eq. 13 and Eq. 16 to approach the FEM solution for the larger distances r from the crack tip.

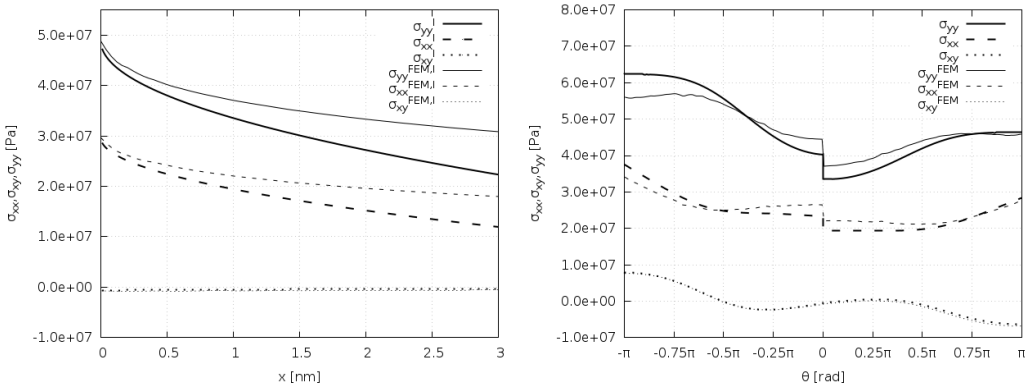

Figure 4: The component of Cauchy stress tensor of the asymptotic solution and FEM solution at the right crack tip.

Materials Research Proceedings 31 (2023) 99-108 https://doi.org/10.21741/9781644902592-11

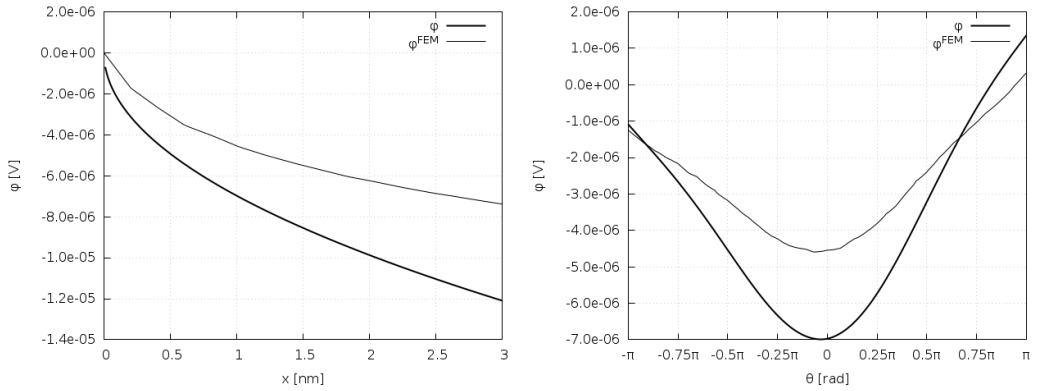

Figure 5: The electric potential of the asymptotic solution and FEM solution at the right crack tip.

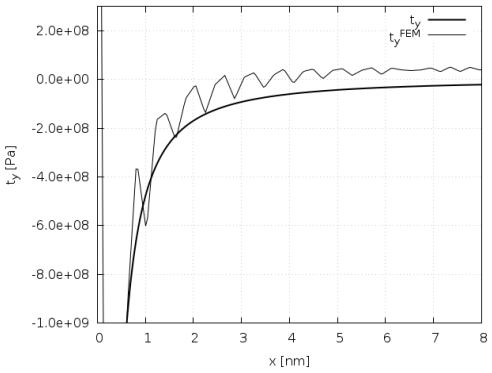

Figure 6: The component $\boldsymbol{t_y}$ of the modified traction vector $\boldsymbol{t}$ of the asymptotic solution and FEM solution ahead of the right crack tip.

The component $t_y = t_y^I = t_y^{II}$ of the modified traction vector $\boldsymbol{t}$ ahead of the crack tip is shown in Fig. 6. The graph depicts the strong singularity $r^{-3/2}$ of $\boldsymbol{t}$ and consequently the failing of the FEM approximation for $r = x \to 0$. Nevertheless, it is seen that the FEM solution becomes to deviate from the analytical solution at $x \approx 1$ nm because of the missing of the higher order terms in the asymptotic solution. Hence the asymptotic solutions Eq. 13 and Eq. 16 describe precisely the singular behavior of the higher order stresses very close to the crack tip and the two-state integral seems to be a very strong tool allowing the extraction of these singular terms from the comprehensive weak solution represented by the FEM.

Summary

The procedure for the assessment of the amplitude factors appearing in the asymptotic solution of the interface crack in flexoelectric bimaterial was discussed. This work follows up and expands the application of the two-state integrals in the fracture mechanics of the material governed by strain gradient elasticity and flexoelectric effect. The obtained results show the ability of the two-state integrals to extract the dominant terms of the asymptotic solution from the weak solution of the fracture problem represented by the FEM. The evaluated amplitude factors of the asymptotic solution are important parameters, which can be used as the inputs to the fracture criterions to predict the interface crack behavior in the flexoelectric materials.

Acknouwledgement

The authors acknowledge the support by the Slovak Science and Technology Assistance Agency registered under number APVV-18-0004, and the support by the Ministry of Education, Science, Research and Sport of the Slovak Republic under grant number VEGA-2/0061/20.

References

[1] P. Yudin, A. Tagantsev, Fundamentals of flexoelectricity in solids, Nanotechnology 24 (2013) 432001. https://doi.org/10.1088/0957-4484/24/43/432001

[2] H. Wang, X. Jiang, Y. Wang, R.W. Stark, van Aken, J. Mannhart, Direct observation of huge flexoelectric polarization around crack tips, Nano Letter 20 (2020) 88-94. https://doi.org/10.1021/acs.nanolett.9b03176

[3] X. Tian, M. Xu, H. Zhou, Q. Li, J. Sladek, V. Sladek, Analytical studies on mode III fracture in flexoelectric solids, Journal of Applied Mechanics 89 (2022) 041006. https://doi.org/10.1115/1.4053268

[4] P.A. Gougiotis, H.G. Georgiadis, Plane-strain crack problems in microstructured solids governed by dipolar gradient elasticity, J. Mech. Phys. Solids 57 (2009) 1898-1920. https://doi.org/10.1016/j.jmps.2009.07.005

[5] F. Vasquez-Sancho, A. Abdollahi, D. Damjanovic, G. Catalan, Flexoelectricity in bones, Advanced Materials 30 (2018) 1705316.

[6] X. Tian, J. Sladek, V. Sladek, Q. Deng, Q. Li, A collocation mixed finite element method for the analysis of flexoelectric solids, Int. J. Solids Struct. 217 (2021) 27-39. https://doi.org/10.1016/j.ijsolstr.2021.01.031

[7] J. Sladek, V. Sladek, M. Hrytsyna, T. Profant, Application of the gradient theory to interface crack between two dissimilar dielectric materials, Engineering Fracture Mechanics 276(B) (2022), 108895. https://doi.org/10.1016/j.engfracmech.2022.108895

[8] F. Deng, Q. Deng, W. Yu, S. Shen, Mixed Finite Elements for Flexoelectric Solids, Journal of Applied Mechanics 84(8) (2017) 081004. https://doi.org/10.1115/1.4036939

[9] J. Sladek, V. Sladek, P. Stanak, C. Zhang, C.-L. Tan, Fracture mechanics analysis of size-dependent piezoelectric solids, Int J Solids Struct 113-114 (2017) 1-9. https://doi.org/10.1016/j.ijsolstr.2016.08.011

[10] M.L. Williams, Stress singularities resulting from various boundary conditions in angular corners of plates in extension, Journal of Applied Mechanics 74 (1952) 526–528.

[11] M. Kotoul, T. Profant, Asymptotic solution for interface crack between two materials governed by dipolar gradient elasticity, Engineering Fracture Mechanics 201 (2018) 80-106. https://doi.org/10.1016/j.engfracmech.2018.05.002

[12] T. Profant, J. Sládek, V. Sládek. M. Kotoul, Asymptotic solution for interface crack between two materials governed by dipolar gradient elasticity: Amplitude factor evaluation, Theoretical and Applied Fracture Mechanics 120 (2022) 103378. https://doi.org/10.1016/j.tafmec.2022.103378

[13] S. Mao, P. K. Purohit, Insights Into Flexoelectric Solids From Strain-Gradient Elasticity, Journal of Applied Mechanics 81(8) (2014) 081004(10). https://doi.org/10.1115/1.4027451